Impact of modified turbulent diffusion of $PM_{2.5}$ aerosol in WRF-Chem simulations in Eastern China

Wenxing Jia[1,2], Xiaoye Zhang[2,3*]

[1]Key Laboratory for Aerosol-Cloud-Precipitation of China Meteorological Administration, Nanjing University of Information Science & Technology, Nanjing, 210044, China

[2]Key Laboratory of Atmospheric Chemistry of CMA, Chinese Academy of Meteorological Sciences, Beijing, 100081, China

[3]Center for Excellence in Regional Atmospheric Environment, IUE, Chinese Academy of Sciences, Xiamen, 361021, China

Correspondence to: X. Zhang (xiaoye@cma.gov.cn)

Abstract

Correct description of the boundary layer mixing process of particle is an important prerequisite to understanding the formation mechanism of pollutants, especially during heavy pollution episodes. Turbulent mixing process of particles is usually denoted by the turbulent diffusion ~~relationship~~ of heat, which is questionable.~~, meaning that the turbulent transport of particles and heat are similar. This similarity has, however, never been verified. Here we investigate the dissimilarity between particles and heat, indicating that the unified treatment of all scalars in the model is questionable.~~ Using mixing-length theory, a new~~the~~ turbulent diffusion relationship of particle is established, embedded in the model and verified on a long-term scale. The new turbulent diffusion coefficient is used to represent the turbulent mixing process of pollutants separately. Simulated results of $PM_{2.5}$ concentration were improved by 8.3% (2013), 17% (2014), 11% (2015) and 11.7% (2017) in Eastern China, respectively. Meanwhile, the new

设置了格式: 字体: 小四, 加粗
设置了格式: 字体: 小四
设置了格式: 字体: 小四, 加粗
设置了格式: 字体: 小四, 加粗
设置了格式: 字体: 小四, 加粗
设置了格式: 字体: 小四
设置了格式: 字体: 小四
设置了格式: 字体: 小四
设置了格式: 字体: 小四

turbulent diffusion does not deteriorate the simulation results of meteorological parameters. Compared with the boundary layer height, turbulent diffusion controls the diffusion of pollutants more significantly. However, under the influence of complex topography, the turbulent diffusion process is insensitive to the simulation of the pollutant concentration. For mountainous area, the evolution of pollutants is more susceptible to advection transport. In addition to the $PM_{2.5}$ concentration, CO as a primary pollutant, its concentration ~~the simulation of the CO concentration~~ has also been improved, which shows that the turbulent diffusion process is extremely critical to ~~the change in the concentration of pollutants~~the variation of the various aerosol pollutants.

设置了格式: 字体: 小四

设置了格式: 字体: 小四

设置了格式: 字体: 小四

设置了格式: 字体: 小四

1 Introduction

Along with the intensive urbanization and tremendous economic development, numerous incidents of aerosol pollution have frequently occurred in China (An et al., 2019; ~~Q. Zhang et al., 2019;~~ X. Zhang et al., 2019). Aerosol pollution, characterized by $PM_{2.5}$, occurs primarily in the planetary boundary layer (PBL). The horizontal transportation and vertical distribution of pollutants are obviously affected by the PBL mixing process, associated with intricate turbulence eddies (~~Liu et al., 2018;~~ Ren et al., 2018; Wang et al., 2018; Du et al., 2020). Turbulent ~~transport~~diffusion, as a vital process, controls the exchange of momentum, heat, water vapor and pollutants through turbulence eddies within the PBL (Stull, 1988).

设置了格式: 字体: 小四

设置了格式: 字体: 小四, 字体颜色: 自动设置

设置了格式: 字体: 小四

设置了格式: 字体: 小四

Moreover, the PBL height (PBLH) directly determines the effective air volume of pollutant diffusion and atmospheric environmental capacity. With the continuous development of technology, there are numerous means (e.g., radiosonde, tethered balloon, meteorological tower, aircraft, ground-based remote sensing and space-based remote sensing) and methods (e.g., based on surface fluxes, Richardson number and others diagnostic methods) to determine the PBLH, of course, the results are also different (Zhang et al., 2020). However, the PBLH is not necessarily negatively

correlated with pollutant concentration (Miao et al., 2021). In particular, turbulence barrier effect can affect the vertical distribution of pollutants (Ren et al., 2021), which make the relationship between pollutant and PBLH more uncertain. The PBLH can also be diagnosed by the boundary layer parameterization schemes in the model, but the PBLH does not directly determine the effective diffusion of pollutants (Jia and Zhang, 2020; Jia et al., 2021a). Instead, the vertical diffusion and mixing of pollutants are directly determined by the turbulent diffusion coefficient (TDC), and the diagnosis of PBLH can affect the calculation of TDC. Previous studies have analyzed some pollution cases by using process analysis methods (Xing et al., 2017; Gao et al., 2018; Chen et al., 2019). The results showed that, for a pollution event, emissions and turbulent diffusion are the two processes that contribute the most to the pollutant concentration. Meanwhile, the contributions of advection transport and chemistry cannot be ignored. The evolution of pollutants is mainly controlled by turbulent diffusion, when emissions are unchanged for a short period. Therefore, more realistic turbulent diffusion characteristics are extremely important for the simulation of pollutant concentration in the model.

~~Turbulent transports of temperature, water vapor and CO_2 has long been considered similar (Kays et al., 2005). However, this statement is usually invalid and is regarded as applicable only under neutral stratifications. Previous researchers have demonstrated that temperature-humidity dissimilarity, and such a disparity between the effectiveness of heat and water vapor transport, is due to different mechanisms of scalar transport (Katul et al., 2008; van de Boer et al., 2014; Guo et al., 2020).For example, the effect of advection (Assouline et al., 2008), entrainment at the top of PBL (Cava et al., 2008; Gao et al., 2018) and heterogeneity in sources and sinks (Detto et al., 2008; Wang et al., 2014; Guo et al., 2016). Moriwaki and Kanda (2006) also indicated that the differences of turbulent transport between heat and CO_2 were due to both by the active role of temperature and the heterogeneity of the source distribution. Li and Bou-Zeid (2011) revealed that the transport dissimilarity between the momentum and the scalar likely resulted from the topology of turbulent structures. As a result, there are differences~~

设置了格式: 字体: 小四

~~between turbulent transport of vectors and scalars, or between scalars. However, less attention has been paid to turbulent transport of particles. Dupont et al. (2019) have proven that the turbulent dissimilarity of transport between dust, heat and momentum. The only studies assumed that particles were considered passive scalars with the same source/sink as heat, and that they used similarity to correct particle flux from the heat flux (Damay et al., 2009; Deventer, Held et al., 2015). A key question is whether the turbulent transport between temperature and particles is similar. This similarity has, however, never been verified, due to the lack of observational turbulence data of particles.~~

To date, there are still some problems need to be solved in the model, especially t~~The t~~urbulent diffusion processes of all scalars (including active and passive scalars) are dealt with in a unified manner in the ~~current~~ mesoscale model. ~~To date, o~~Only a few studies have shown that pointed out the meteorological fields and pollutants can be changed by adjusting the minimum value of TDC~~turbulent diffusion coefficient (TDC)~~ (Savijarvi et al., 2002; Wang et al., 2018; Du et al., 2020; Liu et al., 2021), increasing turbulent kinetic energy (TKE) (Foreman and Emeis, 2012) and modifying experiment expressions (Sušelj and Sood, 2010; Huang and Peng, 2017). Recently, Jia et al. (2021b) obtained the TDC of particles by using high-resolution vertical flux data of particles based on the mixing length theory. Additionally, this relationship has been embedded into the WRF-Chem model to calculate the PBL mixing process of pollutants separately. This work has initially improved the overestimation of pollutant concentration at night in winter 2016 in Eastern China. However, a series of heavy pollution incidents have occurred and attracted much attention since 2013 (~~Yang et al., 2018; Zhong et al., 2019~~Miao et al., 2019). Therefore, we conducted a series of simulations for the heavy pollution periods in winter from 2013 to 2017 in this study. The difference between this study and previous work is that previous work focused on the analysis of observations, while this study mainly explores the influence~~uncertainty~~ of ~~the influence of the model on the~~ turbulent diffusion ~~of particles~~on pollutant concentration in the mesoscale model.

设置了格式: 字体: 小四

设置了格式: 字体: 小四

设置了格式: 字体: 小四

设置了格式: 字体: 小四

设置了格式: 字体: 小四

2 Data and methods

2.1 Data

In this study, the aerosol pollution level is denoted by the hourly surface $PM_{2.5}$ concentration that is available from the official website of the China National Environmental Monitoring Center from 1 January 2013 to 31 January 2017. $PM_{2.5}$ concentration stations increased from 35 cities in 2013(illustrated by red dots in Fig. 1b) to 78 cities in 2017(illustrated by black dots in Fig. 1b) in Eastern China. In addition to $PM_{2.5}$ observations, the hourly concentrations of CO were acquired from the National Air Quality real-time publication platform (http://106.37.208.233:20035, last access: 20 May 2021). ~~Aside from this~~Meanwhile, the hourly meteorological observation data, including temperature, pressure, relative humidity, wind and visibility from the national automatic weather stations (AWS) provided by the National Meteorological Information Center of China Meteorological Administration (NMICMA) (illustrated by gray crosses in Fig. 1b). The time period of the data selected is from 1 January 2013 to 31 January 2017. In addition, the turbulent diffusion of particles is calculated using high-frequency turbulence data, and observational turbulence data are obtained from the Pingyuan County Meteorological Bureau (37.15°N, 116.47°E), Shandong Province, China from 27 December 2018 to 8 January 2019 (illustrated by orange triangle in Fig. 1b). Identical eddy-covariance systems were operated, including three-dimensional sonic anemometer-thermometer (IRGASON, Campbell Scientific, USA) and CO_2/H_2O open-path gas analyzer (LI7500, LI-COR, USA). These instruments measured three components of wind speed, potential temperature, water vapor and CO_2 concentrations with a frequency of 10 Hz. The turbulence data finally was split into 30-min segments. ~~In addition, a~~A continuous particle measuring instrument E-sampler (Met One) and a high-frequency sampling visibility sensor CS120A (Campbell Scientific, USA) were used to obtain $PM_{2.5}$ mass concentration every minute and visibility of 1 Hz. The calculation of 30-min vertical flux of $PM_{2.5}$ is based on the nonlinear relationship between $PM_{2.5}$ concentration and visibility (Ren et al., 2020). Detailed background and

设置了格式: 字体: 小四
设置了格式: 字体: 小四
设置了格式: 字体: 小四
设置了格式: 字体: 小四
设置了格式: 字体: 小四
设置了格式: 字体: 小四
设置了格式: 字体: 小四
设置了格式: 字体: 小四
设置了格式: 字体: 小四, 下标
设置了格式: 字体: 小四

calculation principle of this method were presented in Ren et al. (2020), so we only describe key steps. Firstly, we separate $PM_{2.5}$ concentration (~~*C*~~ *c*) and visibility datasets (*V*) into mean and turbulent deviations (i.e., $c=\bar{c}+c'$ and $V=\bar{V}+V'$). Secondly, we get the fitted coefficients by using exponential correlation (i.e., *a* and *b*) between the $PM_{2.5}$ concentration and visibility (i.e., $c=a\cdot V^{b}$). Thirdly, combining the first two steps, we can get the turbulent fluctuations of $PM_{2.5}$ concentration (i.e., $c'=a\cdot(\bar{V}+V')^{b}-\bar{c}$). Finally, we use fluctuations of vertical velocity (i.e., *w'*) and of *PM2.5* concentration (i.e., *c'*) to calculate the vertical flux of $PM_{2.5}$ (i.e., $\overline{w'c'}$).

To ~~investigate~~ illustrate the influence of the PBL height (PBLH) on the $PM_{2.5}$ pollution, soundings collected at the Fuyang site (32.54°N,115.5°E) and the Anqing site (30.37° N,116.58°E) (illustrated by yellow pluses in Fig. 1b) for the period 2013-2017 were analyzed. These two stations are equipped with L-band radiosonde systems (~~Miao et al., 2018~~Jia et al., 2021c), which proved a fine resolution (1 Hz) profiles of temperature, relative humidity and wind speed two times (0800 and 2000 BJT) a day during winter. To eliminate the error caused by the difference of calculation methods of PBLH, Richardson number method is used to calculate the PBLH in both observation and simulation. The Richardson number is defined as follows:

$$Ri(z)=\frac{g\left(\theta_{vz}-\theta_{vs}\right)\left(z-z_{s}\right)}{\theta_{vs}\left(u_{z}-u_{s}\right)^{2}+\left(v_{z}-v_{s}\right)^{2}} \quad (1)$$

where *z* is the height above ground, g is the gravity, θ_v is the virtual potential temperature, and *u* and *v* are the component of wind. The subscript "s" denotes the surface level. The height at which the Richardson number equals 0.25 is defined as the PBLH, which is consistent with the definition of simulation.~~,~~

设置了格式: 字体: 倾斜
设置了格式: 字体: 小四, 倾斜
设置了格式: 字体: 小四
设置了格式: 字体: 小四
设置了格式: 字体: 小四
设置了格式: 字体: 倾斜
设置了格式: 字体: 倾斜
设置了格式: 字体: 小四
设置了格式: 字体: 小四
设置了格式: 字体: 小四
设置了格式: 字体: 小四, 倾斜
设置了格式: 字体: 小四
设置了格式: 字体: 小四
设置了格式: 字体: 小四
设置了格式: 字体: 小四
设置了格式: 字体: 小四
设置了格式: 字体: 小四

2.2 Numerical simulation

Long-term three-dimensional simulation experiments are enforced using the Weather Research and Forecasting model coupled with Chemistry (WRF-Chem version 3.9.1) (Grell et al., 2005) in this study from the winter of 2013 to 2017, when Eastern China frequently experienced severe and persistent aerosol pollution events ~~(Zhong et al., 2019)~~. One month for each winter from 2013 to 2017 was selected, and a total of four months were confirmed, which are January 2013, December 2014, December 2015 and January 2017, respectively. The anthropogenic emissions of BC, OC, CO, NH_3, NO_x, $PM_{2.5}$, PM_{10} and volatile organic compounds (VOCs) are set based on the latest monthly Multi-resolution Emission Inventory for China (MEIC) from 2013 to 2017 are provided by Tsinghua University, with a resolution of 0.25°×0.25° (http://meicmodel.org/, last access: 20 May 2021). The model domain was centered over Eastern China with a horizontal resolution of 33 and 6.6 km (Fig. 1a). The model top was set to the 50 hPa level, and 48 vertical layers were configured below the top. To resolve the PBL structure, 21 vertical layers were set below 2 km (Above Ground Level, AGL) ~~were set~~. The physics parameterization schemes selected for this study included the Morrison double-moment microphysics scheme (Morrison et al., 2009), RRTMG longwave/shortwave radiation schemes (Iacono et al., 2008), MM5 similarity surface layer scheme (Jiménez et al., 2012), Noah land surface scheme (Chen and Dudhia, 2001), Singer-layer UCM scheme (Kusaka et al., 2001), CLM4.5 lake physics scheme (Subin et al., 2012; Gu et al., 2015), ACM2 planetary boundary layer scheme (Pleim, 2007), Grell-3D cumulus scheme (Grell and Devenyi, 2002). And the chemical mechanism is the RADM2-MADE/SORGM scheme (Ackermann et al., 1998; Schell et al., 2001). The initial and boundary conditions of meteorological fields were set up using the National Centers for Environmental Prediction (NCEP) global final (FNL) reanalysis data, with a resolution of 1°×1° (https://rda.ucar.edu/datasets/ds083.2/, last access: 20 May 2021). And the initial and boundary conditions of chemical fields were configured using the global model output of Model for Ozone and Related Chemical

设置了格式: 字体: 小四
设置了格式: 字体: 小四
设置了格式: 字体: 小四
设置了格式: 字体: 小四
设置了格式: 字体: 小四
设置了格式: 字体: 小四
设置了格式: 字体: 小四
设置了格式: 字体: 小四
设置了格式: 字体: 小四
设置了格式: 字体: 小四

Tracers (MOZART) (http://www/acom.ucar.edu/wrf-chem/mozart.shtml, last access: 20 May 2021).

Simulation using abovementioned configurations is referred to as the original runs. In the original PBL parameterization scheme, TDCs of heat and momentum are different (i.e., $K_h \neq K_m$), T the turbulent mixing process of pollutants is considered to be similar to that of heat, which supposes the eddy turbulent diffusions of particles and heat are identical (i.e., $K_h=K_c$). While in the improved scheme, the eddy turbulent diffusion mixing process of particles pollutants is calculated by the TDC of particles (i.e., K_c), which is different from that TDC of heat (i.e., $K_{he} \neq K_{ch}$). These improved experiments are regarded as the new runs hereafter. All simulation included a total of eight months. The 91-h simulation is conducted beginning from 0000UTC of three days ago for each day (i.e., 248 simulation experiments), and first 64-h of each simulation is considered as the spin-up period.

2.3 Calculation principle of turbulent diffusion of particles

Considering that the pollution is usually accompanied by the stable boundary layer (SBL), and the simulation results of pollutant concentration are poor in the SBL at night. Thus, we mainly modify the program of the stable boundary layer, while for the unstable boundary layer, we still use the default program of the original scheme.

The TDC is parameterized by the mixing length (l) and the function of Richardson number ($f(Ri)$) based on Mixing length theory, that is

$$K = 0.01 + \sqrt{ss} \cdot l^2 \cdot f(Ri) \quad (2)$$

where ss is the wind shear (i.e., $ss = (\partial u/\partial z)^2 + (\partial v/\partial z)^2$), 0.01 refers to the minimum value of TDC in the model, T and the mixing length formula (i.e., $l = \kappa z/(1+\kappa z/\lambda)$, λ ~~λ~~=80) proposed by Blackadar (1962), and it is widely used in the model (Louis, 1979; ~~Liu and Carroll, 1996;~~ Lin et al., 2008; Pleim, 2016). Many previous studies have

设置了格式: 字体: 小四
设置了格式: 字体: 小四
设置了格式: 字体: 小四
设置了格式: 字体: 小四
设置了格式: 字体: 小四
设置了格式: 字体: 小四
设置了格式: 字体: 小四
带格式的: 标题 2
设置了格式: 字体: 四号
设置了格式: 字体: 小四
设置了格式: 字体: 小四
带格式的: 缩进: 首行缩进: 0.85 厘米, 段落间距段后: 0 磅
设置了格式: 字体: 小四
设置了格式: 字体: 小四
设置了格式: 字体: 小四
设置了格式: 字体: 小四
设置了格式: 字体: 小四
设置了格式: 字体: 小四

showed various functions of Richardson number, which represent the different situations of turbulence. Here, we mainly compare the similarities and differences between the turbulent diffusion of momentum, heat and particles in the model.

(i) For the stable conditions (i.e., $Ri \geq 0$), Esau and Byrkjedal (2007) suggested:

$$f_h = (1+10Ri+50Ri^2+5000Ri^4)^{-1}+0.0012 \quad (3)$$

$$f_m = 0.8 f_h + 0.00104 \quad (4)$$

where f_h and f_m denote the functions of heat and momentum, respectively, and these functions have been implemented in the original model. We added an additional function of particles into the model, that is

$$f_c = (1+66.6Ri)^{-1} \quad (5)$$

which is used to denote the turbulent mixing process of particles within the PBL. When Ri is greater than ~0.2, the TDC of particles is greater than that of heat, which may reduce pollutant concentration. With the increase of instability, the TDC of particles is gradually smaller than that of heat, which theoretically leads to the increase of pollutant concentration. For detailed analysis and comparison of functions, please refer to Jia et al. (2021b).

(ii) For the unstable conditions (Ri<0)~~, Equation (2) is rewritten as~~:

$$f_h = f_c = (1-25Ri)^{1/2} \quad (6)$$

$$f_m = \mathrm{Pr} \cdot f_h \quad (7)$$

where the TDC of particles is still equal to that of heat, while the TDC of momentum is calculated by turbulent Prandtl number (i.e., Pr, Pr=0.8).

~~Considering that the pollution is usually accompanied by the stable boundary layer, we mainly modify the program of the stable boundary layer, while for the unstable boundary layer, we still use the default program of the original scheme.~~

There are several important ~~things to note~~information about the TDC of particles that need to be illustrated. (1) ~~It is~~Turbulent diffusion of particles calculated by the explicit local gradient to represent the PBL mixing process of particles, which are more suitable

设置了格式: 字体: 小四

设置了格式: 字体: 小四, 倾斜
设置了格式: 字体: 小四
带格式的: 段落间距段后: 0 磅
带格式的: 缩进: 首行缩进: 0.85 厘米, 段落间距段后: 0 磅
设置了格式: 字体: 小四
设置了格式: 字体: 小四
带格式的: 缩进: 首行缩进: 0.85 厘米, 段落间距段后: 0 磅
设置了格式: 字体: 小四
设置了格式: 字体: 小四
带格式的: 段落间距段后: 0 磅
设置了格式: 字体: 小四
设置了格式: 字体: 小四
设置了格式: 字体: 小四
域代码已更改
带格式的: 缩进: 首行缩进: 0.85 厘米, 段落间距段后: 0 磅
设置了格式: 字体: 小四
设置了格式: 字体: 倾斜
设置了格式: 字体: 小四
设置了格式: 字体: 小四
设置了格式: 字体: 小四
带格式的: 缩进: 首行缩进: 0.85 厘米, 段落间距段后: 0 磅
带格式的: 缩进: 首行缩进: 0.85 厘米, 段落间距段后: 0 磅
设置了格式: 字体: 小四
设置了格式: 字体: 小四
带格式的: 缩进: 首行缩进: 0.85 厘米, 段落间距段后: 0 磅
带格式的: 缩进: 首行缩进: 0.85 厘米, 段落间距段后: 0 磅
设置了格式: 字体: 小四
设置了格式: 字体: 小四
设置了格式: 字体: 小四
设置了格式: 字体: 小四

in the stable boundary layer (SBL) (Mahrt and Vickers, 2003). (2) The new scheme avoids the inapplicability of the Monin-Obukhov similarity theory (MOST), the deviation of the PBLH in the SBL, and higher computational efficiency (Li et al., 2010), and it is easier to applied to the forecasting models in the future. (3) It Turbulent diffusion of particles is used to evaluate the PBL mixing process of pollutants separately, which can improve affect the simulation results of pollutants and does not deteriorate influence the simulation results of meteorological parameters.

设置了格式: 字体: 小四

设置了格式: 字体: 小四

设置了格式: 字体: 小四

设置了格式: 字体: 小四

设置了格式: 字体: 小四

设置了格式: 字体: 小四

3 Temperature-particles transport dissimilarity

The $PM_{2.5}$ concentration frequently reached hazardous levels above 100 μg m^{-3} during six heavy pollution episodes (marked by HPE1-HPE6 in Fig. S1). The turbulent characteristics of $PM_{2.5}$ concentration have been demonstrated in Ren et al. (2020), and the turbulence characteristics of heat and particles were markedly different (Jia et al., 2021; Ren et al., 2021). Based on the previous studies, the turbulent correlation coefficient is used to evaluate the transport efficiencies for heat, water vapor, momentum and particles (Stull, 1988; Li and Bou-Zeid, 2011; Dupont and Patton, 2012). The expression as follows:

$$R_{wp}=\frac{\overline{w'p'}}{\sigma_w\sigma_p} \quad (8)$$

R_{wp} denotes the correlation coefficient between the fluctuations of *w'* and *p'*, while *p* stands for the temperature *T*, specific humidity *q*, longitudinal velocity component *u* and particles *c*. This value is between -1 to 1 (negative correlation to positive correlation), and zero indicates that the two parameters are uncorrelated. The σ_w and σ_p are the standard deviations of vertical velocity and parameter *p* (i.e., *T*, *q*, *u*, *c*) over a 30-min interval, respectively. If the MOST is applicable, it indicates the turbulent mechanisms of heat, water vapor and particles are the same, i.e., $R_{wt}=R_{wq}=R_{wc}$ (Liu et al., 2017). Previous studies have investigated different mechanisms of scalar transport between temperature and humidity (Moriwaki and Kanda 2006; Katul et al., 2008; van de Boer et al., 2014; Guo et al., 2016, 2020). Lacking profile data for the $PM_{2.5}$ concentration (Yuan et al., 2019; Ren et al., 2020), there is little about the transport efficiency of fine particles (i.e., $PM_{2.5}$). The correlation coefficient of heat flux and particle flux can be defined as:

$$R_{wt,wc} = \frac{\overline{\left(w't' - \overline{w't'}\right)\left(w'c' - \overline{w'c'}\right)}}{\sigma_{w't'}\sigma_{w'c'}} \quad (9)$$

$\sigma_{w't'}$ and $\sigma_{w'c'}$ are the standard deviations of $w't'$ and $w'c'$, respectively. The correlation coefficients of the heat (R_{wt}), fine particles (R_{wc}), and heat flux and particle flux ($R_{wt,wc}$) are presented in Fig. 2. Clearly, there is an obvious difference between R_{wt} and R_{wc}. Whether transport efficiency is R_{wt} or R_{wc}, transport efficiency can exhibit the greatest variability at night during the HPEs, probably suggesting an increasing complexity of turbulent structures at night (Fig. 2b and 2c). High correlation exists between heat and fine particles fluxes at night (especially at the wee hours) in the HPEs (Fig. 2d), which indicates that these fluxes are performed by the same motions within the PBL. Previous research has noted that the atmospheric vertical mixing is mainly controlled by the large-scale eddies' percentage at night during the HPEs (Li et al., 2020). However, it should be mentioned that the correlation coefficient between heat and fine particles fluxes ($R_{wt,wc}$) changes dramatically at night (Fig. 2d). This means that these two fluxes transported with different eddies in a short time, or transported at different time periods by the same eddy when the correlations diminish. Consequently, there is a difference between the transport of heat and fine particles fluxes. Whether scalar is temperature or particle, it is debatable that the mixing process of all scalars are dealt with a unified manner within the PBL. As a result, we urgently need to develop a TDC of particles, which is used only to calculate the mixing process of pollutants within the PBL.

34 Improvement Evaluation of $PM_{2.5}$ concentration simulation

Based on the TDC relationship of particles in the previous study (Jia et al., 2021b), this study applies this relationship to a long-term scale simulation for verification. Figure 23 shows the average value of simulated and observed $PM_{2.5}$ concentration at night from 2013 to 2017, and the simulation results can better reproduce the distribution of pollutant concentration (i.e., represented by the red dashed circle). However, the $PM_{2.5}$ concentration was overestimated into varying degrees in Eastern China (i.e., indicated by the green dashed circle),. and The mean relative bias (RB) in of the mean regional value is as high as 11.8% (2013), 48% (2014), 23.8% (2015) and 20.9% (2017), respectively (Fig. 23i-l). In addition, we also found that the pollutant concentrations are

设置了格式: 字体: 小四
设置了格式: 字体: 小四
设置了格式: 字体: 小四
设置了格式: 字体: 小四
设置了格式: 字体: 小四
设置了格式: 字体: 小四
设置了格式: 字体: 小四

underestimated in Beijing (BJ) and along the Taihang Mountains (Mt. Taihang) (i.e., indicated by the purple irregular circle), but overestimated in Tianjin (TJ) (Fig. 2i-l). What are the reasons for the pollutant concentration simulated by the same model are different in various regions? What are the different effects of turbulent diffusion in various regions? These issues will be further explained later, and this section mainly evaluates the simulation results of the pollutant concentration. Compared to the original scheme, the new scheme improves the situation where the pollutant concentration is overestimated at night in Eastern China (Fig. 34a-d). The degree of overestimation of the pollutant concentration is reduced, and the mean relative bias ~~of average value~~ of the new scheme is 3.5% (2013), 31% (2014), 12.8% (2015) and 9.2% (2017), respectively (Fig. 34e-h). Moreover, the mean absolute bias ~~in the mean value~~ is reduced by 8.3% (2013), 17% (2014), 11% (2015) and 11.7% (2017), respectively (Fig. ~~4i~~3j-l). In summary, compared with the original scheme, the new scheme can generally improve the overestimation of pollutant concentration in Eastern China, which is due to the improvement of turbulent diffusion. For the previously mentioned stations where underestimated the pollutant concentration in the original scheme, the pollutant concentration will be further underestimated with the increase of turbulent diffusion. However, this underestimation cannot be avoided because there is an opposite phenomenon in the pollutant concentration of the two regions. We can only look at the differences in the two regions from other perspectives (see section 4 for details), due to there are many uncertainties in the model.

To better evaluate the model performance, F~~f~~igure 45 shows the Taylor diagram of hourly $PM_{2.5}$ concentration, and the black (red) dots indicate original (new) simulation results at all stations from 2013 to 2017. The statistical results present a consistent feature, that is, the worse the simulation results of the original scheme are, the more obvious improvement of the new scheme becomes (arrows indicate improved stations in the Fig. 45). The results indicate that the pollutant concentrations at all stations are not improved to the same extent. When the simulation of pollutant concentration is overestimated by the original scheme ~~overestimates the pollutant concentrations~~, the

设置了格式: 字体: 小四
设置了格式: 字体: 小四
设置了格式: 字体: 小四
设置了格式: 字体: 小四
设置了格式: 字体: 11 磅
设置了格式: 字体: 小四
设置了格式: 字体: 小四
设置了格式: 字体: 小四

new scheme will significantly reduce the degree of overestimation. While the simulation of pollutant concentrations ~~are~~ is underestimated by the original scheme, the new scheme ~~does not increase the degree of underestimation again (Fig. 5)~~will not further underestimate with the previous changing and the degree of re-underestimate is not obvious (Fig. 4). And the standard deviation (normalized) of the mean value is decreased by 0.2 (2013), 0.28 (2014), 0.14 (2015) and 0.16 (2017) (Fig. ~~4~~5). As a whole, the new scheme can significantly improve the common phenomenon of overestimated pollutant concentration in the SBL in Eastern China (Fig. ~~4~~5).

With the increase of turbulent diffusion, the pollutant concentration decreases gradually. Where do the reduced pollutants go? Did it spread to the surrounding area in the horizontal direction or to the upper level in the vertical direction? This question deserves further discussion. It can be seen from Figure 3 that the reduction of pollutant concentration is a regional synchronous change, and there is no regular concentration gradient in the horizontal direction. Therefore, ~~In addition to the changes in the pollutant concentration near the surface,~~ we should also pay more attention to the changes ~~in the pollutant concentration~~ in the vertical direction. Theoretically, increasing turbulent diffusion will reduce the pollutant concentrations near the surface-layer, and the pollutants will be more fully mixing in the vertical direction, which results in lower concentrations of pollutants in the near surface-layer and higher concentrations of pollutants in the upper layer. ~~Actually~~As we expected, the pollutant concentration is reduced in the surface-layer and it is increased in the upper layer at night (Fig. ~~5~~6), which is consistent with the theory.

~~4~~5 Uncertainty analysis

~~4~~5.1 Meteorological parameters

Depending on ~~the transport dissimilarity of heat and particles~~high-frequency particle flux, the TDC of particles ~~was~~ has been added ~~separately~~ in the model to calculate the

设置了格式: 字体: 小四
设置了格式: 字体: 小四
设置了格式: 字体: 小四
设置了格式: 字体: 小四
设置了格式: 字体: 小四
设置了格式: 字体: 小四
设置了格式: 字体: 小四
设置了格式: 字体: 小四

turbulent mixing process of particles separately. Compared with previous studies on the improvement of parameterization scheme, the greatest strengths of the new scheme are that not only improves the simulation results of pollutant concentration, but also does not deteriorate the simulation results of other parameters. ~~For correctional approaches, it is important that a new scheme does not lead to worse performance than that with the original scheme.~~ To verify the new scheme ~~without affecting~~does not affect the simulation results of the meteorological parameters, the simulation results of the near-surface meteorological elements (i.e., 2-m temperature, 2-m relative humidity and 10-m wind speed) between original and new schemes have been compared and analyzed. It can be seen from Figure S1~~2~~-S34 that the correlation coefficients of meteorological parameters by two schemes are greater than 0.99, noting that the new scheme does not alter the performance of meteorological fields, which is an advantage of the new scheme. ~~Compared with previous studies~~As mentioned earlier, modifying the turbulent diffusion coefficient of heat not only affects the simulation of temperature (Savijarvi and Kauhanen, 2002), but also influences the results of pollutants (Liu et al., 2021). Improving the parameterization scheme is a long and tough process, making it difficult to improve the simulation results of all parameters at once. When the simulation results of one parameter are improved, we should first seek to ensure that the simulation results of other parameters are not deteriorated. Then, we are going to look at improving other parameters. Although the aerosol-radiation two-way feedback process has been considered in the ~~atmospheric chemistry two-way coupled~~ WRF-Chem model, the ~~mean fractional change in~~change of $PM_{2.5}$ concentration caused by radiation feedback is only ~~varying just~~ a few percentage (Li et al., 2017; Wu et al., 2019; Gao et al., 2020). We should focus more on the feedback process between turbulence and aerosol, and hopefully develop a turbulence-aerosol two-way feedback module. Some turbulent characteristics (e.g., turbulence barrier effect) can be taken into consideration during ~~the~~ HPEs, reflecting a more realistic ~~pollutant concentration~~ evolution process of pollutant concentration. We ~~think the next step is to solve this major problem.~~ will further clarify the relationship between particles, momentum and heat transport through observational data, so as to lay the foundation for the improvement of the model.

设置了格式: 字体: 小四

设置了格式: 字体: 小四

设置了格式: 字体: 小四

设置了格式: 字体: 小四

设置了格式: 字体: 小四

设置了格式: 字体: 小四

设置了格式: 字体: 小四

设置了格式: 字体: 小四

45.2 PBL height

Although PBL height (PBLH) is widely used to determine the effective air volume and atmospheric environmental capacity for pollutant diffusion ~~(Miao et al., 2018), the influence of PBLH on the pollution is uncertain. (1) There are various methods to determine the PBLH, either through observation or simulation (Jia and Zhang., 2020; Zhang et al., 2020).~~ vVarious methods diagnose different PBLH, which reinforces uncertainty about the PBLH as a criterion. ~~(2) There does not necessarily reflect a negative correlation between pollutant concentration and PBLH. The relationship between the PBLH and $PM_{2.5}$ pollution has been revealed on the basis of the four-year radiosonde measurements, and the results show that the correlation between PBLH and $PM_{2.5}$ concentration is different in various regions (Miao et al., 2018). Moreover, when the PBLH is higher, the corresponding pollutant concentration is not necessarily lower (Miao et al., 2021).~~ When there is a transport stage ~~during the HPEs~~ with a high wind speed during HPEs, the mechanical turbulence is strong, and the PBLH and pollutant concentration increase simultaneously (Jia et al., 2021c; Miao et al. 2021). Therefore, the relationship between PBLH and $PM_{2.5}$ pollution is intricate. The impact of PBLH is ultimately represented through the TDC in the model, because the PBLH is used to calculate TDC (Jia et al., 2021b), and~~,~~ artificial changing PBLH can also affect the simulation of pollutant concentration. If the simulation error of pollutant concentration is ~~clearly controlled by the PBLH~~caused by the PBLH, ~~when~~ that is the pollutant concentration is overestimated and the PBLH ~~is to~~should be underestimated. However, the PBLH is reproduced well by the model, and the model does not underestimate the PBLH (Fig. ~~6~~7). Anqing is located in the mountain corridor, the simulation results of PBLH (Index of agreement, IOA=0.49~0.81) is slightly worse than that in Fuyang (IOA=0.63~0.85). Therefore, various factors will influence the calculation of PBLH. A more accurate PBLH can indeed reduce some uncertainty of the model, but how to apply the accurate PBLH through observation to the model is a thorny problem. For example, the turbulence barrier effect changes the mixing height of pollutants (Ren et al., 2021), which cannot be reflected in the model and can lead to deviation in the

设置了格式: 字体: 小四
设置了格式: 字体: 小四
设置了格式: 字体: 小四
设置了格式: 字体: 小四
设置了格式: 字体: 小四
设置了格式: 字体: 小四
设置了格式: 字体: 小四
设置了格式: 字体: 小四
设置了格式: 字体: 小四

simulation of pollutant concentration. The new scheme does not disturb the simulation results of meteorological fields, ~~and therefore~~thus, does not affect the simulation results of PBLH (Fig. S~~4~~5). The simulation results of ~~the simulation of~~ pollutant concentrations are improved under the similar PBLH, which further demonstrates that the simulation of pollutant concentration is not only controlled by the PBLH, but also influenced by turbulent diffusion. In the final analysis, turbulent diffusion controls the diffusion of pollutant concentration and the evolution of meteorological parameters.~~—~~

~~4~~5.3 Influence of other processes

Overestimating of pollutant concentrations has been improved in Eastern China, but there are also some sites in northern China where pollutant concentrations are underestimated (Fig. 2i-l). These sites (i.e., Hebei and Beijing) are mostly located in the east of the Taihang Mountains and the south of the Yan Mountains (Fig. 7~~8~~). For example, in December 2016, the pollutant concentrations of all sites in Beijing were not underestimated. Jia et al. (2021b) have found that the pollutant concentrations of two sites located in the south of Beijing (i.e., blue dots in Fig. S2 in Jia et al., 2021b) are well reproduced by the model ~~(i.e., away from the mountain)~~. This phenomenon also occurred in 2013-2017 (Fig. 7~~8~~), and the pollutant concentrations were significantly underestimated at some sites, which are close to the mountainous area ~~(i.e., near the mountain)~~. The boundaries of overestimated and underestimated sites are pronounced in Beijing-Tianjin-Hebei region (white dashed in Fig. 7~~8~~), and the pollutant concentration is overestimated at some sites, which are away from the mountainous area (i.e., Tianjin and southeast of Hebei). Meanwhile, the TDC of the new scheme is greater than that of the original scheme in Eastern China (i.e., red dashed circle in Fig. 8i-l), that is, the increased turbulent diffusion reduces the overestimation of pollutant concentration in this area. Furthermore, we found that the TDC of ~~particles in~~ the new scheme is significantly smaller than t~~he TDC~~hat of ~~heat in~~ the original scheme in the mountainous area (i.e., green irregular circle in Fig. 8~~red rectangle in Fig. S6~~). ~~The terrain will disturb the turbulence fields, making the stable stratification weakly~~

设置了格式: 字体: 小四
设置了格式: 字体: 小四
设置了格式: 字体: 小四
设置了格式: 字体: 小四
设置了格式: 字体: 小四
设置了格式: 字体: 小四
设置了格式: 字体: 小四
设置了格式: 字体: 小四
设置了格式: 字体: 小四
设置了格式: 字体: 小四
设置了格式: 字体: 小四
设置了格式: 字体: 小四

~~stable/unstable.~~ Theoretically, the reduced TDC ~~will~~ should increase the pollutant concentration~~ near the mountain~~, and improve the underestimation of pollutant concentration in~~of~~ the original scheme. ~~However~~Disappointingly, the change of TDC does not improve the underestimation of pollutant concentration in the mountainous area (Fig. 7, 8i-l), which ~~shows~~ indicates that the change of turbulent diffusion is not sensitive to the pollutant concentration in the mountainous area.~~impact of other processes is more obvious in the mountain area.~~

In addition to the two main influencing factors of emission and turbulent diffusion, advection transport and chemistry processes can also affect the simulation of pollutant concentration. Since we use the latest emissions source inventory, there is no way to use other more elaborate inventories to quantify the uncertainty caused by emissions. ~~For instance, the a~~Advection process is ~~strongly~~ highly related to ~~the~~ wind and ~~pollutant~~ $PM_{2.5}$ concentration gradients from upwind areas to downwind areas (Gao et al., 2018). Figure 9~~S7~~ shows that the simulation results of wind speed, and we found that the wind speed is overestimated in the whole simulation area, which is also the systematic deviation of the model (Jia and Zhang, 2020). However, there are regional differences in the overestimation of wind speed, which is more obvious in areas with complex terrain (framed by purple lines in Fig. 9). Jimenez and Dudhia (2012) indicated that the overestimation of wind speed may be caused by the incorrect describe sub-grid surface roughness. For the purple rectangle region, although the wind speed is overestimated, there is no obvious wind speed gradient and pollutant concentration gradient (Fig. 2a-d, 9a-d). Thus, the effect of advection is not significant. While for the irregular purple region, we can see that the obvious wind speed gradient and pollutant concentration gradient (Fig. 2a-d, 9a-d). In the northwest of the irregular purple area, clean air will pass through this area under the control of stronger northwesterly wind. Therefore, this area is extremely likely to be affected by advection transport, so that the pollutant concentration has been underestimated in this area. We should pay more attention to the improvement of wind field simulation on complex terrain and we expect that the simulation of wind field will be improved and the pollutant concentration in

设置了格式: 字体: 小四
设置了格式: 字体: 小四
设置了格式: 字体: 小四
设置了格式: 字体: 小四
设置了格式: 字体: 小四
设置了格式: 字体: 小四
设置了格式: 字体: 小四
设置了格式: 下标
设置了格式: 字体: 小四

this area will also be improved. ~~the wind speed is much more overestimated in the mountain areas (two purple rectangles in Fig. S7i-l), but only the pollutant concentration is always underestimated in the BTH region (Fig. 3i-l). Clear gradients of wind speed and pollutant concentration exist in the BTH region (Fig. 3a-d; Fig. S7a-d), so these sites (i.e., closer to the mountain) may be significantly affected by the advection process. Hence, the influences of other processes or topography in the mountain area deserve further consideration in the future.~~

Chemistry process, i.e., the $PM_{2.5}$ concentration contribution caused by secondary transformation, was negligible in this study, and is not mentioned further in this paper. Whether the simulation of chemical components has been improved, it cannot be well verified ~~because of the~~due to lack of observational data. Although the ~~observational~~ simulation results of ~~components of~~ $PM_{2.5}$ components are not ~~available to evaluate the simulation results of new scheme~~capable of being evaluated, CO, as a representative of primary pollutants, can be compared to the observations. Results from new scheme with TDC of particles are more consistent with the observations than the original scheme (Fig. S~~5~~8), which supports the improvement of $PM_{2.5}$ concentration (Fig. 4~~5~~ and S~~5~~8). In addition, the dry deposition process of particles is also extremely important (Zhang et al., 2001; Farmer et al., 2021). The turbulent mixing and dry deposition processes belong to the same main program in the mesoscale model. However, with increasing particle size, particle inertia and gravity cannot be neglected, but these inertia and gravity effects are neglected for particles smaller than 10 μm in diameter (Fratini et al., 2007). Therefore, we did not involve the influence of gravity on pollutant concentration in this study. In the future, we should use long-term simulation results to verify the difference of aerosol process decomposition in detail.

设置了格式: 字体: 小四

设置了格式: 字体: 小四

设置了格式: 字体: 小四

设置了格式: 字体: 小四

设置了格式: 字体: 小四

5~~6~~ Conclusions and prospects

At present, m~~M~~esoscale model ~~faces~~ is facing numerous challenges, especially during ~~the~~ heavy pollution ~~events~~episodes. One of these challenges is the correct describe

设置了格式: 字体: 小四

设置了格式: 字体: 小四

设置了格式: 字体: 小四

~~description of~~ the turbulent mixing process of pollutants. Although the model can reproduce the evolution of pollutants, the simulation of ~~the~~ diurnal variation of pollutants is fundamentally flawed, especially at night. Errors in estimation of pollutant concentration are primarily caused by defects in the turbulent mixing of pollutants in the model. Actually, there is a difference between the turbulent transport of heat and particles. This result inspires us to deal with the turbulent diffusion of heat and particles separately. Therefore, based on the turbulent diffusion expression of particles proposed by Jia et al., 2021b, we again ~~audited~~ demonstrated the improvement of pollutant concentration in winter from 2013 to 2017, and the uncertainty factors are also analyzed in the model.~~.~~

The original scheme overestimates the surface $PM_{2.5}$ concentration by 11.8% (2013), 48% (2014), 23.8% (2015) and 20.9% (2017) at night, respectively. The new scheme has improved the overestimation of the surface $PM_{2.5}$ concentration in eastern China at night, and the ~~average~~ mean absolute bias of ~~average value~~the region can be reduced by 8.3% (2013), 17% (2014), 11% (2015) and 11.7% (2017), respectively. In the horizontal direction, the pollutant concentration showed regional synchronous changes. ~~In the vertical direction, the pollutant concentration is decreased in the surface layer while it increased in the upper layer.~~Therefore, the pollutant concentration is reduced near the surface and better mixed in the whole layer, increasing the pollutant concentration in the upper level. Moreover, the new scheme not only improves the simulation of pollutant concentration, but also does not deteriorate the simulation of other meteorological parameters. ~~improvement of the pollutant concentration field does not interfere with changing meteorological fields.~~Although the PBLH affects the diffusion of pollutants, the simulation of pollutant concentration is not specifically controlled by the PBLH, but effected by TDC. It is worth noting that ~~However,~~ TDC has a negligible impact on the simulation of pollutant concentration at some sites with complex topography. Meanwhile, advection transport may dominate the evolution of pollutant concentration in mountainous area. The simulation results of $PM_{2.5}$ components cannot be ~~used to~~ evaluated, ~~the results of the simulation of the new scheme,~~ due to ~~the~~ lack of

设置了格式: 字体: 小四
设置了格式: 字体: 小四
设置了格式: 字体: 小四
设置了格式: 字体: 小四
设置了格式: 字体: 小四
设置了格式: 字体: 小四
设置了格式: 字体: 小四

observational data. CO, however, as a representative of primary pollutants, can be compared to observations. Results from new scheme are more consistent with the observations than the original scheme, which supports the improvement of $PM_{2.5}$ concentration.

The new scheme could provide promising guidance during ~~the~~ heavy pollution ~~events~~episodes. The turbulent transport mechanism and ~~scalar~~ turbulent parameterization is a complex topic (~~Smedman et al., 2007,~~ Lemon et al., 2019; Couvreux et al., 2020; Edwards et al., 2020), and beyond that, other processes (or other parameters) also need in-depth understanding and exploration (Zhang et al., 2001; Seinfeld et al., 2016; Shao et al., 2019; Emerson et al., 2020). Therefore, more research during the heavy pollution ~~events~~episodes, especially on the experimental side (e.g., carry out extensive measurement campaigns), might shed more light on the turbulent mixing process and transport mechanisms of pollutants ~~and their mechanisms~~.

设置了格式: 字体: 小四
设置了格式: 字体: 小四
设置了格式: 字体: 小四
设置了格式: 字体: 小四
设置了格式: 字体: 小四
设置了格式: 字体: 小四
设置了格式: 字体: 小四
设置了格式: 字体: 小四

Data availability

The surface $PM_{2.5}$ concentration, meteorological data, turbulent datasets and turbulent flux data of $PM_{2.5}$ are available by request (xiaoye@cma.gov.cn).

设置了格式: 字体: 小四

Author contributions

Development of the ideas and concepts behind this work was performed by all the authors. Model execution, data analysis and paper preparation were performed by WJ and XZ with feedback and advice.

设置了格式: 字体: 小四

Competing interests

The authors declare that they have no conflict of interest.

设置了格式: 字体: 小四

Acknowledgments

The authors would like to acknowledge the Tsinghua University for the support of emission data.

设置了格式: 字体: 小四

Financial support

This research is supported by the Major Program of the NSFC Project (42090031); ~~This research is supported by the~~ NSFC Project (U19A2044); ~~National Key Project of MOST (2016YFC0203306); Atmospheric Pollution Control of the Prime Minister Fund (DQGG0104); Key Projects of Fundamental Scientific Research Fund of CAMS (2017Z001).~~

References

Ackermann, I. J., Hass, H., Memmesheimer, M., Ebel, A., Binkowski, F. S., and Shankar, U.: Modal aerosol dynamics model for Europe, Atmos. Environ., 32, 2981–2999, https://doi.org/10.1016/S1352-2310(98)00006-5, 1998.

An, Z., Huang, R., Zhang, R., Tie, X., Li, G., Cao, J., Zhou, W., Shi, Z., Han, Y., Gu, Z., and Ji, Y.: Severe haze in northern China: A synergy of anthropogenic emissions and atmospheric processes, P. Natl. Acad. Sci. USA, 116, 8657–8666, https://doi.org/10.1073/pnas.1900125116, 2019.

~~Assouline, S., Tyler, S. W., Tanny, J., Cohen, S., Bou-Zeid, E., Parlange, M. B., and Katul, G. G.: Evaporation from three water bodies of different sizes and climates: measurements and scaling analysis, Adv. Water Resour., 31, 160–172, https://doi.org/10.1016/j.advwatres.2007.07.003, 2008.~~

Blackadar, A. K.: The vertical distribution of wind and turbulent exchange in a neutral atmosphere, J. Geophys. Res., 67, 3095–3102, https://doi.org/10.1029/JZ067i008p03095, 1962.

~~Cava, D., Katul, G. G., Sempreviva, A. M., Giostra, U., and Scrimieri, A.: On the anomalous behaviour of scalar flux-variance similarity functions within the canopy sub-layer of a dense alpine forest, Bound. Lay. Meteorol., 128, 33–57, https://doi.org/10.1007/s10546-008-9276-z, 2008.~~

Chen, F., and Dudhia, J.: Coupling an advanced land surface – hydrology model with the Penn State – NCAR MM5 modeling system. Part I: model implementation and sensitivity, Mon. ~~Weather~~ Wea. Rev., 129, 569–585, https://doi.org/10.1175/1520-0493(2001)129 < 0587:CAALSH > 2.0.CO, 2, 2001.

Chen, L., Zhu, J., Liao, H., Gao, Y., Qiu, Y., Zhang, M., Liu, Z., Li, N., and Wang, Y.: Assessing the formation and evolution mechanisms of severe haze pollution in the Beijing–Tianjin–Hebei region using process analysis, Atmos. Chem. Phys., 19, 10845-10864, https://doi.org/10.5194/acp-19-10845-2019, 2019.

Couvreux, F., Bazile, E., Rodier, Q., Maronga, B., Matheou, G., and Chinita, M. J., Edwards, J., Stratum, B. J. H., van Heerwaarden, C. C., Huang, J., Moene, A. F., Cheng, A., Fuka, V., Basu, S., Bou-Zeid, E., Canut, G., and Vignon, E.: Intercomparison of large-eddy simulations of the Antarctic boundary layer for very stable stratification, Bound.-Lay. Meteorol., 176, 369–400, https://doi.org/10.1007/s10546-020-00539-4, 2020.

Damay, P. E., Maro, D., Coppalle, A., Lamaud, E., Connan, O., Hébert, D., Tallbaut, M., and Irvine, M.: Size-resolved eddy covariance measurements of fine particle vertical fluxes, J. Aerosol Sci., 40, 1050–1058, https://doi.org/10.1016/j.jaerosci.2009.09.010, 2009.

Detto, M., Katul, G., Mancini, M., Montaldo, N., and Albertson, J. D.: Surface heterogeneity and its signature in higher-order scalar similarity relationships, Agric. For. Meteorol., 148, 902–916, https://doi.org/10.1016/j.agrformet.2007.12.008, 2008.

Deventer, M. J., El Madany, T., Griessbaum, F., and Klemm, O.: One-year measurement of size-resolved particle fluxes in an urban area, Tellus B: Chem. Phys. Meteorol., 67, 25531, https://doi.org/10.3402/tellusb.v67.25531, 2015.

Du, Q., Zhao, C., Zhang, M., Dong, X., Cheng, Y., Liu, Z., Hu, Z., Zhang, Q., Li, Y., Yuan, R., and Miao, S.: Modeling diurnal variation of surface $PM_{2.5}$ concentrations over East China with WRF-Chem: impacts from boundary-layer mixing and anthropogenic emission, Atmos. Chem. Phys., 20, 2839–2863, https://doi.org/10.5194/acp-20-2839-2020, 2020.

Dupont, S., and Patton, E. G.: Momentum and scalar transport within a vegetation canopy following atmospheric stability and seasonal canopy changes: The CHATS experiment, Atmos. Chem. Phys., 12, 5913–5935, https://doi.org/10.5194/acp-12-5913-2012, 2012.

Dupont, S., Rajot, J. L., Labiadh, M., Bergametti, G., Lamaud, E., Irvine, M. R., Alfaro, S. C., Bouet, C., Fernandes, R., Khalfallah, B., Marticorena, B., Bonnefond, J. M., Chevaillier, S., Garrigou, D., Henry-des-Tureaux, T., Sekrafi, S., and Zapf, P.: Dissimilarity between dust, heat and momentum turbulent transports during Aeolian soil erosion, J. Geophys. Res.-Atmos., 124, 1064–1089, https://doi.org/10.1029/2018JD029048, 2019.

Edwards, J. M., Beijaars, A. C., Holtslag, A. A., and Lock, A. P.: Representation of boundary-layer processes in numerical weather prediction and climate models, Bound.-Lay. Meteorol., 177, 511–539, https://doi.org/10.1007/s10546-020-00530-z, 2020.

Emerson, E. W., Hodshire, A. L., Debolt, H. M., Bilsback, K. R., Pierce, J. R., McMeeking, G. R., and Farmer, D. K.: Revisiting particle dry deposition and its role in radiative effect estimates, P. Natl. Acad. Sci. USA, 117, 26076–26082, https://doi.org/10.1073/pnas.2014761117, 2020.

Esau, I. N., and Byrkjedal, Ø.: Application of large eddy simulation database to optimization of first order closure for neutral and stably stratified boundary layers, Bound.-Lay. Meteorol., 125, 207–225, https://doi.org/10.1007/s10546-007-9213-6, 2007.

Farmer, D.K., Boedicker, E.K. and DeBolt, H.M.: Dry Deposition of Atmospheric Aerosols: Approaches, Observations, and Mechanisms, Annu. Rev. Phys. Chem. 72, 16.1–16.23, https://doi.org/10.1146/annurev-physchem-090519-034936, 2021.

Foreman, R. J., and Emeis, S.: A Method for Increasing the Turbulent Kinetic Energy in the Mellor–Yamada–Janjić Boundary-Layer Parametrization, Bound.-Lay. Meteorol., 145, 329–349, https://doi.org/10.1007/s10546-012-9727-4, 2012.

Fratini, G., Ciccioli, P., Febo, A., Forgione, A., and Valentini, R.: Size-segregated fluxes of mineral dust from a desert area of northern China by eddy covariance. Atmos. Chem. Phys., 7, 2839–2854, https://doi.org/10.5194/acp-7-2839-2007, 2007.

Gao, J., Zhu, B., Xiao, H., Kang, H., Pan, C., and Wang, D., and Wang, H.: Effects of black carbon and boundary layer interaction on surface ozone in Nanjing, China, Atmos. Chem. Phys., 18, 7081–7094, https://doi.org/10.5194/acp-18-7081-2018, 2018.

Gao, M., Han, Z., Tao, Z., Li, J., Kang, J.-E., Huang, K., Dong, X., Zhuang, B., Li, S., Ge, B., Wu, Q., Lee, H.-J., Kim, C.-H., Fu, J. S., Wang, T., Chin, M., Li, M., Woo, J.-H., Zhang, Q., Cheng, Y., Wang, Z., and Carmichael, G. R.: Air quality and climate change, Topic 3 of the Model Inter-Comparison Study for Asia Phase III (MICS-Asia III) – Part 2: aerosol radiative effects and aerosol feedbacks, Atmos. Chem. Phys., 20, 1147–1161, https://doi.org/10.5194/acp-20-1147-2020, 2020.

~~Gao, Z., Liu, H., Li, D., Katul, G. G., and Blanken, P. D.: Enhanced temperature-humidity similarity caused by entrainment processes with increased wind shear, J. Geophys. Res. Atmos., 123, 4110–4121, https://doi.org/10.1029/2017JD028195, 2018.~~

Grell, G. A., and Devenyi, D.: A generalized approach to parameterizing convection combining ensemble and data assimilation techniques, Geophys. Res. Lett., 29, 1693, https://doi.org/10.1029/2002GL015311, 2002.

Grell, G.A., Peckham, S.E., Schmitz, R., McKeen, S.A., Frost, G., Skamarock, W.C., and Eder, B.: Fully coupled "online" chemistry within the WRF model. Atmos. Environ., 39, 6957–6975. https://doi.org/10.1016/j.atmosenv.2005.04.027, 2005.

Gu, H., Jin, J., Wu, Y., Ek, M. B., and Subin, Z. M.: Calibration and validation of lake surface temperature simulations with the coupled WRF-lake model, Clim. Change., 129, 471–483, https://doi.org/10.1007/s10584-013-0978-y, 2015.

Guo, X., Sun, Y., and Miao, S.: Characterizing urban turbulence under haze pollution: insights into temperature humidity dissimilarity, Bound. Lay. Meteorol., 158, 501–510, https://doi.org/10.1007/s10546-015-0104-y, 2016.

Guo, X., Yang, K., Yang, W., Zhao, L., Li, S., and Ding, B.: Representing the heat-to-moisture transport efficiency in stable conditions: an extension of two different approaches, Asia-Pac. J. Atmos. Sci., 56, 603–611, https://doi.org/10.1007/s13143-019-00155-4, 2020.

Huang, Y., and Peng, X.: Improvement of the Mellor–Yamada–Nakanishi–Niino Planetary Boundary-Layer Scheme Based on Observational Data in China, Bound.-Lay. Meteorol., 162, 171–188, https://doi.org/10.1007/s10546-016-0187-0, 2017.

Iacono, M. J., Delamere, J. S., Mlawer, E. J., Shephard, M. W., Clough, S. A., and Collins, W. D.: Radiative forcing by long-lived greenhouse gases: calculations with the AER radiative transfer models, J. Geophys. Res.: -Atmos., 113, D13103. https://doi.org/10.1029/2008JD009944, 2008.

Jia, W., and Zhang, X.: The role of the planetary boundary layer parameterization schemes on the meteorological and aerosol pollution simulations: A review, Atmos. Res., 239, 104890, https://doi.org/10.1016/j.atmosres.2020.104890, 2020.

Jia, W., Zhang, X., and Wang, Q.: Assessing the pollutant evolution mechanisms of heavy pollution episodes in the Yangtze-Huaihe valley: A multiscale perspective, Atmos. Environ., 244, 117986, https://doi.org/10.1016/j.atmosenv.2020.117986, 2021a.

Jia, W., Zhang, X., Zhang, H., and Ren, Y.: Application of turbulent diffusion term of aerosols in mesoscale model, Geophys. Res. Lett., 48, e2021GL093199, https://doi.org/10.1029/2021GL093199, 2021b.

Jia, W., Zhang, X., Wang, J., Yang, Y., and Zhong, J.: The influence of stagnant and transport types weather on heavy pollution in the Yangtze-Huaihe valley, China, Sci. Total Environ., 792, 148393, https://doi.org/10.1016/j.scitotenv.2021.148393, 2021c.

域代码已更改

Jiménez, P.A., Dudhia, J.: Improving the representation of resolved and unresolved topographic effects on surface wind in the WRF model, J. Appl. Meteorol. Climatol., 51, 300–316, https://doi.org/10.1175/JAMC-D-11-084.1, 2012.

Jiménez, P. A., Dudhia, J., González–Rouco, J. F., Navarro, J., Montávez, J. P., and García–Bustamante E.: A revised scheme for the WRF surface layer formulation, Mon. Wea. Rev., 140, 898–918, https://doi.org/10.1175/MWR-D-11-00056.1, 2012.

Katul, G. G., Sempreviva, A. M., and Cava, D.: The temperature-humidity covariance in the marine surface layer: a one-dimensional analytical model, Bound.-Lay. Meteorol., 126, 263–278, https://doi.org/10.1007/s10546-007-9236-z, 2008.

Kays, W. M., Crawford, M. E., and Weigand, B.: Convective heat and mass transfer, McGraw-Hill Higher Education, Boston, 2005.

Kusaka, H., Kondo, H., Kikegawa, Y., and Kimura, F.: A simple single-layer urban canopy model for atmospheric models: comparison with multi-layer and slab models. Bound.-Lay. Meteorol., 101, 329–358, https://doi.org/10.1023/a:1019207923078, 2001.

LeMone, M. A., Angevine, W. M., Bretherton, C. S., Chen, F., Dudhia, J., Fedorovich, E., Katsaros, K. B., Lenschow, D. H., Mahrt, L., Patton, E. G, Sun, J. L., Tjernström, M., and Weil, J.: 100 Years of progress in boundary layer meteorology, Meteorol. Mono., 59, 9.1–9.85, https://academic.microsoft.com/paper/2935666247, 2019.

Li, D., and Bou-Zeid, E.: Coherent structures and the dissimilarity of turbulent transport of momentum and scalars in the unstable atmospheric surface layer, Bound.-Lay. Meteorol., 140, 243–262, https://doi.org/10.1007/s10546-011-9613-5, 2011.

Li, M., Wang, T., Xie, M., Zhuang, B., Li, S., Han, Y., and Chen, P.: Impacts of aerosol-radiation feedback on local air quality during a severe haze episode in Nanjing megacity, eastern China, Tellus B: Chem. Phys. Meteorol., 69, 1339548, https://doi.org/10.1080/16000889.2017.1339548, 2017.

Li, X., Gao, C. Y., Gao, Z., and Zhang, X.: Atmospheric boundary layer turbulence structure for severe foggy haze episodes in north China in December 2016, Environ. Pollut., 264, 114726, https://doi.org/10.1016/j.envpol.2020.114726, 2020.

Li, Y., Gao, Z., Lenschow, D. H., and Chen, F.: An improved approach for parameterizing surface-layer turbulent transfer coefficients in numerical models, Bound.-Lay. Meteorol., 137, 153–165, https://doi.org/10.1007/s10546-010-9523-y, 2010.

Lin, J., Youn, D., Liang, X., and Wuebbles, D. J.: Global model simulation of summertime U.S. ozone diurnal cycle and its sensitivity to PBL mixing, spatial resolution, and emissions, Atmos. Environ., 42, 8470–8483, https://doi.org/10.1016/j.atmosenv.2008.08.012, 2008.

Liu, C., Huang, J. Hu, X.-M., Hu, C., Wang, Y., Fang, X., Luo, L., Xiao, H., and Xiao, H.: Evaluation of WRF-Chem simulations on vertical profiles of $PM_{2.5}$ with UAV observations during a haze pollution event, Atmos. Environ., 252, 118332, https://doi.org/10.1016/j.atmosenv.2021.118332, 2021.

Liu, M., Lin, J., Wang, Y., Sun, Y., Zheng, B., and Shao, J., Chen, L., Zheng, Y., Chen, J., Fu, T. M., Yan, Y., Zhang, Q., and Wu, Z.: Spatiotemporal variability of NO_2 and $PM_{2.5}$ over Eastern China: observational and model analyses with a novel statistical method, Atmos. Chem. Phys., 18, 12933–12952, https://doi.org/10.5194/acp-18-12933-2018, 2018.

Liu, M., and Carroll, J. J.: A high-resolution air pollution model suitable for dispersion studies in complex terrain, Mon. Wea. Rev., 124, 2396–2409, https://doi.org/10.1175/1520-0493(1996)124<2396:ahrapm>2.0.co;2, 1996.

Liu, Y., Liu, H., Wang, L. The vertical distribution characteristics of integral turbulence statistics in the atmospheric boundary layer over an urban area in Beijing. Science China Earth Sciences, 60, 1533–1545, https://doi.org/10.1007/s11430-016-9050-5, 2017

Louis, J.: A parametric model of vertical eddy fluxes in the atmosphere, Bound.-Lay. Meteorol., 17, 187–202, https://doi.org/10.1007/BF00117978, 1979.

Mahrt, L., and Vickers, D.: Formulation of turbulent fluxes in the stable boundary layer, J. Atmos. Sci., 60, 2538–2548, https://doi.org/10.1175/1520-0469(2003)060<2538:FOTFIT>2.0.CO;2, 2003.

Miao, Y., Che, H., Zhang, X., and Liu, S.: Relationship between summertime concurring $PM_{2.5}$ and O_3 pollution and boundary layer height differs between Beijing and Shanghai, China, Environ. Pollut., 268, 115775, https://doi.org/10.1016/j.envpol.2020.115775, 2021.

Miao, Y., Li, J., Miao, S., Che, H., Wang, Y., Zhang, X., Zhu, R., and Liu, S.: Interaction between planetary boundary layer and PM2.5 pollution in megacities in China: a review, Curr. Pollut. Rep., 5, 261–271, https://doi.org/10.1007/s40726-019-00124-5, 2019.

Miao, Y., Liu, S., Guo, J., Huang, S., Yan, Y., and Lou, M.: Unraveling the relationships between boundary layer height and $PM_{2.5}$ pollution in China based on four-year radiosonde measurements, Environ. Pollut., 243, 1186-1195, https://doi.org/10.1016/j.envpol.2018.09.070, 2018.

~~Moriwaki, R., and Kanda, M.: Local and global similarity in turbulent transfer of heat, water vapour, and CO2 in the dynamic convective sublayer over a suburban area, Bound. Lay. Meteorol., 120, 163–179, https://doi.org/10.1007/s10546-005-9034-4, 2006.~~

Morrison, H., Thompson, G., and Tatarskii, V.: Impact of Cloud Microphysics on the Development of Trailing Stratiform Precipitation in a Simulated Squall Line: Comparison of One– and Two–Moment Schemes, Mon. Wea. Rev., 137, 991–1007, https://doi.org/10.1175/2008MWR2556.1, 2009.

Pleim, J. E.: A combined local and nonlocal closure model for the atmospheric boundary layer. Part I: model description and testing, J. Appl. Meteorol. Climatol., 46, 1383–1395, https://doi.org/10.1175/JAM2539.1, 2017.

Pleim, J. E., Gilliam, R., Appel, W., and Ran, L.: Recent advances in modeling of the atmospheric boundary layer and land surface in the coupled WRF-CMAQ model, Air Pollution Modeling and its Application XXIV, 391–396, https://doi.org/10.1007/978-3-319-24478-5_64, 2016.

Ren, Y., Zhang, H., Wei, W., Cai, X., and Song, Y.: Determining the fluctuation of $PM_{2.5}$ mass concentration and its applicability to Monin–Obukhov similarity, Sci. Total Environ., 710, 136398, https://doi.org/10.1016/j.scitotenv.2019.136398, 2020.

Ren, Y., Zhang, H., Zhang, X., Wei, W., Li, Q., Wu, B., Cai, X., Song, Y., Kang, L., and Zhu, T.: Turbulence barrier effect during heavy haze pollution events, Sci. Total Environ., 753, 142286, https://doi.org/10.1016/j.scitotenv.2020.142286, 2021.

~~Ren, Y., Zhang, H., Zhang, X., Li, Q., Cai, X., Song, Y., Kang, L., and Zhu, T.: Temporal and spatial characteristics of turbulent transfer and diffusion coefficient of $PM_{2.5}$, Sci. Total Environ., 782, 146804, https://doi.org/10.1016/j.scitotenv.2021.146804, 2021.~~

Ren, Y., Zheng, S., Wei, W., Wu, B., Zhang, H., Cai, X., and Song, Y.: Characteristics of the turbulent transfer during the heavy haze in winter 2016/17 in Beijing, J. Meteor. Res., 32, 69–80, https://doi.org/10.1007/s13351-018-7072-3, 2018.

Savijärvi, H., and Kauhanen, J.: High resolution numerical simulations of temporal and vertical variability in the stable wintertime boreal boundary layer: a case study, Theor. Appl. Climaol., 70, 97–103, https://doi.org/10.1007/s007040170008, 2002.

Schell, B., Ackermann, I. J., and Hass, H.: Modeling the formation of secondary organic aerosol within a comprehensive air quality model system, J. Geophys. Res., 106, 28275–28293, https://doi.org/10.1029/2001JD000384, 2001.

Seinfeld, J. H., Bretherton, C., Carslaw, K. S., Coe, H., DeMott, P. J., Dunlea, E. J., Feingold, G., Ghan, S., Guenther, A. B., Kahn, R., Kraucunas, I., Kreidenweis, S. M., Molina, M. J., Nenes, A., Penner, J. E., Prather, K. A., Ramanathan, V., Ramaswamy, V., Rasch, P. J., Ravishankara, A. R., Rosenfeld, D., Stephens, G., and Wood, R.: Improving our fundamental understanding of the role of aerosol-cloud interactions in the climate system, P. Natl. Acad. Sci. USA, 113, 5781–5790. https://doi.org/10.1073/pnas.1514043113, 2016.

Shao, J., Chen, Q, Wang, Y., Lu, X., He, P., Sun, Y., Shah, V., Martin, R. V., Philip, S., Song, S., Zhao, Y., Xie, Z., Zhang, L., and Alexander, B.: Heterogeneous sulfate aerosol formation mechanisms during wintertime Chinese haze events: air quality model assessment using observations of sulfate oxygen isotopes in Beijing, Atmos. Chem. Phys., 19, 6107–6123. https://doi.org/10.5194/acp-19-6107-2019, 2019.

Smedman, A.-S., Högström, U., Hunt, J. C. R., and Sahlée, E.: Heat/mass transfer in the slightly unstable atmospheric surface layer, Q. J. R. Meteorol. Soc. 133, 37–51. https://doi.org/10.1002/qj.7, 2007.

Stull, R. B.: An introduction to boundary layer meteorology, Atmospheric Sciences Library, 6, 206–210, 1988.

Subin, Z. M., Riley, W. J., and Mironov, D.: An improved lake model for climate simulations: Model structure, evaluation, and sensitivity analyses in CESM1, J. Adv. Model. Earth Syst., 4, M02001, https://doi.org/10.1029/2011MS000072, 2012.

Sušelj, K., and Sood, A.: Improving the Mellor–Yamada–Janjić Parameterization for wind conditions in the marine planetary boundary layer, Bound.-Lay. Meteorol., 136, 301–324. https://doi.org/10.1007/s10546-010-9502-3, 2010.

~~van de Boer, A., Moene, A. F., Graf, A., Schüttemeyer, D., and Simmer, C.: Detection of entrainment influences on surface layer measurements and extension of Monin–Obukhov similarity theory, Bound. Lay. Meteorol.,152:19–44, https://doi.org/10.1007/s10546-014-9920-8, 2014.~~

~~Wang, L., Li, D., Gao, Z., Sun, T., Guo, X., and Bou-Zeid, E.: Turbulent transport of momentum and scalars above an urban canopy, Bound.-Lay. Meteorol., 150:485–511, https://doi.org/10.1007/s10546-013-9877-z, 2014.~~

Wang, H., Peng, Y., Zhang, X., Liu, H., Zhang, M., Che, H., Cheng, Y., and Zheng, Y.: Contributions to the explosive growth of $PM_{2.5}$ mass due to aerosol-radiation feedback and decrease in turbulent diffusion during a red alert heavy haze in Beijing-Tianjin-Hebei, China, Atmos. Chem. Phys. 18, 17717–17733. https://doi.org/10.5194/acp-18-17717-2018, 2018.

Wu, J., Bei, N., Hu, B., Liu, S., Zhou, M., Wang, Q., Li, X., Liu, L., Feng, T., Liu, Z., Wang, Y., Cao, J., Tie, X., Wang J., Molina, L. T., and Li, G.: Aerosol–radiation feedback deteriorates the wintertime haze in the North China Plain, Atmos. Chem. Phys., 19, 8703–8719, https://doi.org/10.5194/acp-19-8703-2019, 2019.

Xing, J., Wang, J., Mathur, R., Wang, S., Sarwar, G., Pleim, J., Hogrefe, C., Zhang, Y., Jiang, J., Wong, D., and Hao, J.: Impacts of aerosol direct effects on tropospheric ozone through changes in atmospheric dynamics and photolysis rates. Atmos. Chem. Phys., 17, 9869 – 9883, https://doi.org/10.5194/acp-17-9869-2017, 2017.

~~Yang, Y., Zheng, X., Gao, Z., Wang, H., Wang, T., Li, Y., Lau, G. N. C., and Yim, S. H. L.: Long-term trends of persistent synoptic circulation events in planetary boundary layer and their relationships with haze pollution in winter half year over eastern China, J. Geophys. Res. Atmos., 123, 10,991–11,007. https://doi.org/10.1029/2018JD028982, 2018.~~

~~Yuan, R., Zhang, X., Liu, H., Gui, Y., Shao, B., and Tao, X., Wang, Y., Zhong, J., Li, Y., and Gao, Z.: Aerosol vertical mass flux measurements during heavy aerosol pollution episodes at a rural site and an urban site in the Beijing area of the North China Plain, Atmos. Chem. Phys., 19, 12857–12874, https://doi.org/10.5194/acp-19-12857-2019, 2019.~~

Zhang, H., Zhang, X., Li, Q., Cai, X., Fan, S., Song, Y., Hu, F., Che, H., Quan, J., Kang, L., and Zhu, T.: Research progress on estimation of the atmospheric boundary layer height, J. Meteor. Res., 34, 482–498, https://doi.org/10.1007/s13351-020-9910-3, 2020.

Zhang,.L, Gong, S., Padro, J., and Barrie, L.: A size-segregated particle dry deposition scheme for an atmospheric aerosol module, Atmos. Environ., 35, 549–560, https://doi.org/10.1016/S1352-2310(00)00326-5, 2001.

~~Zhang, Q., Zheng, Y., Tong, D., Shao, M., Wang, S., Zhang, Y., Xu, X., Wang, J., He, H., Liu, W., Ding, Y., Lei, Y., Li, J., Wang, Z., Zhang, X., Wang, Y., Cheng, J., Liu, Y., Shi, Q., Yan, L., Geng, G., Hong, C., Li, M., Liu, F., Zheng, B., Cao, J., Ding, A., Gao, J., Fu, Q., Huo, J., Liu, B., Liu, Z., Yang, F.,~~

域代码已更改

He, K., and Hao, J.: Drivers of improved $PM_{2.5}$ air quality in China from 2013 to 2017, P. Natl. Acad. Sci. USA, 116, 24463–24469. https://doi.org/10.1073/pnas.1907956116, 2019.

Zhang, X., Xu, X., Ding, Y., Liu, Y., Zhang, H., Wang, Y., and Zhong, J.: The impact of meteorological changes from 2013 to 2017 on $PM_{2.5}$ mass reduction in key regions in China, Sci. China Earth Sci., 62, 1–18. https://doi.org/10.1007/s11430-019-9343-3, 2019.

Zhong, J., Zhang, X., Wang, Y., Wang, J., Sheng, X., Zhang, H., Wang, T., Xie, Z., Liu C., Zhang, H., Zhao, T., Sun, J., Fan, S., Gao, Z., Li, Y., and Wang, L.: The two-way feedback mechanism between unfavorable meteorological conditions and cumulative aerosol pollution in various haze regions of China, Atmos. Chem. Phys., 19, 3287–3306, https://doi.org/10.5194/acp-19-3287-2019, 2019.

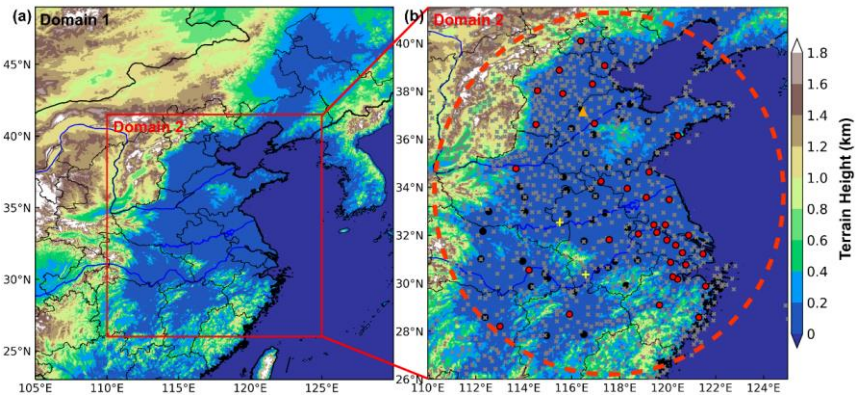

Figure 1. (a) Map of terrain height in the two nested model domains. (b) The locations of surface meteorological stations, air quality monitoring stations and sounding stations are marked by the gray crosses, red(black) dots and yellow pluses, respectively. The turbulence data site is denoted by the orange triangle. The red dashed circle indicates the areas of our primary concern.

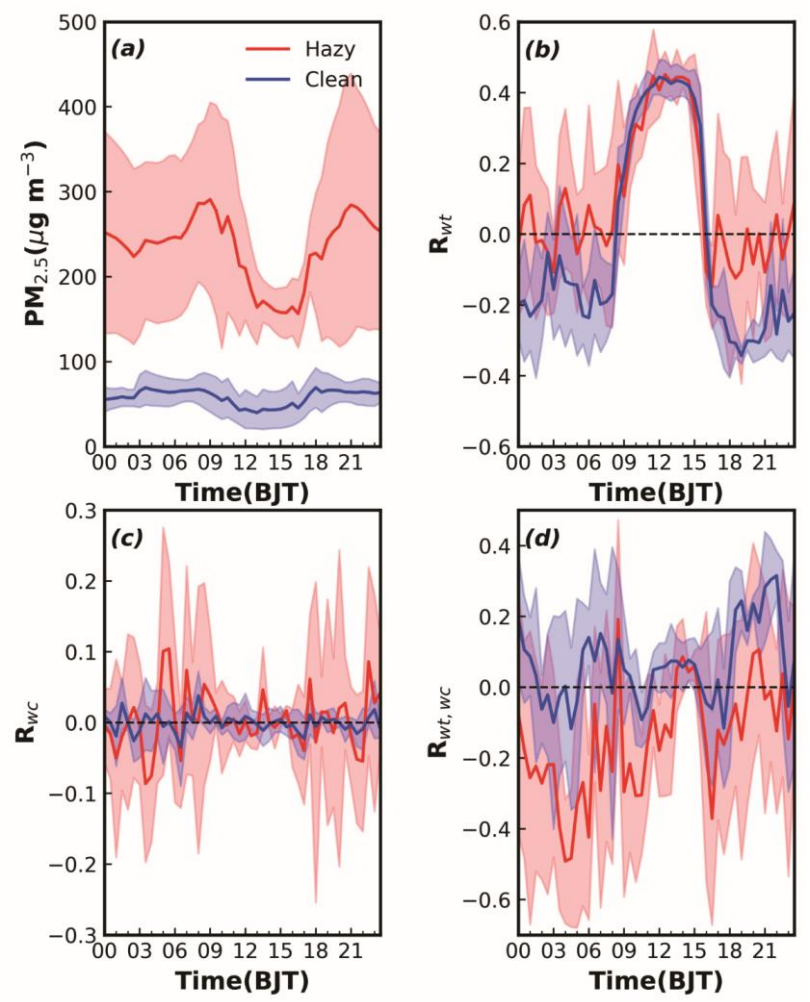

~~**Figure 2. Diurnal variations of (a) $PM_{2.5}$ concentration, (b) transport efficient of heat flux (R_{wt}), (c) transport efficient for fine particles flux (R_{wc}) and (d) correlations of heat and fine particles fluxes ($R_{wt,wc}$). The red (blue) line represents the heavy (cleaning) pollution episodes, and the shaded area indicates the average value ± standard deviation.**~~

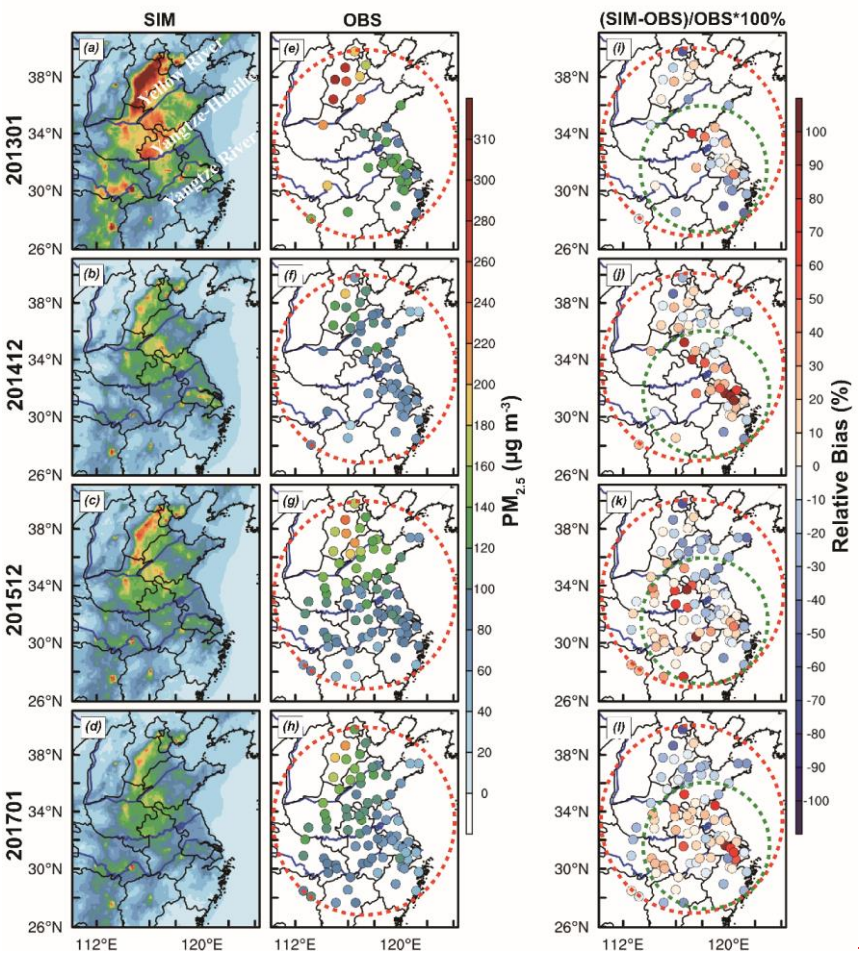
SIM
OBS
(SIM-OBS)/OBS*100%
201301
201412
201512
201701
(a)
(b)
(c)
(d)
(e)
(f)
(g)
(h)
(i)
(j)
(k)
(l)
Yellow River
Huaihe River
Yangtze River
38°N
34°N
30°N
26°N
112°E
120°E
PM2.5 (μg m-3)
310
300
280
260
240
220
200
180
160
140
120
100
80
60
40
20
0
Relative Bias (%)
100
90
80
70
60
50
40
30
20
10
0
-10
-20
-30
-40
-50
-60
-70
-80
-90
-100

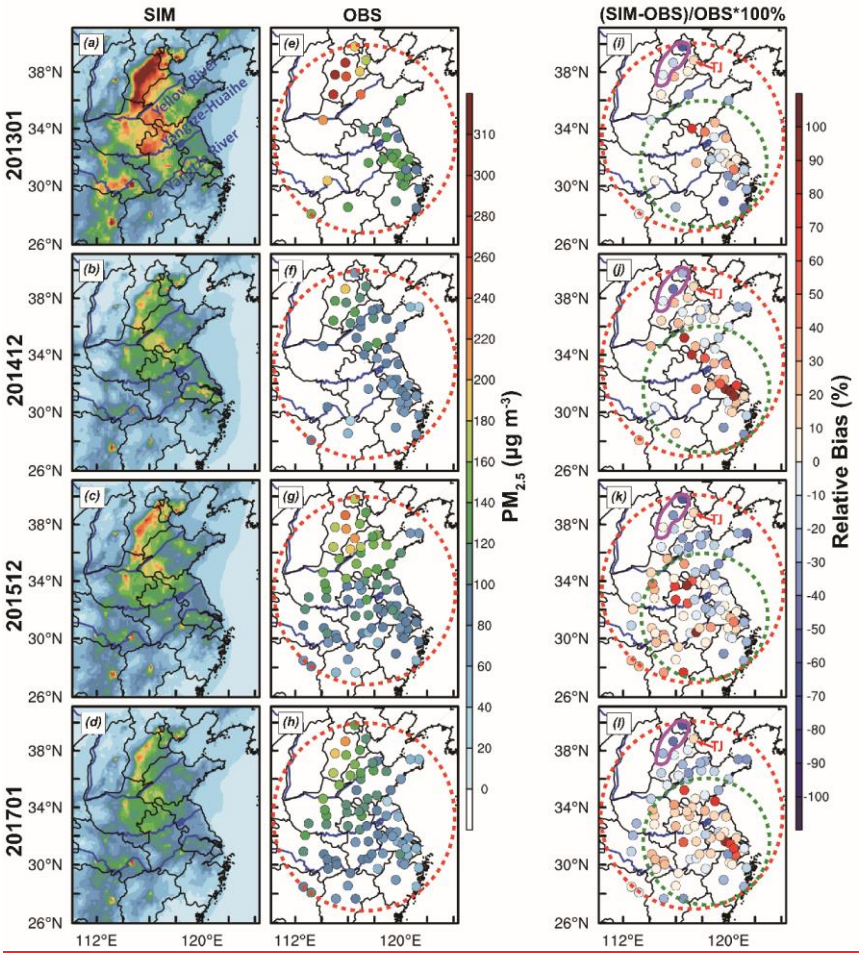

Figure 2~~3~~. The average value of (a-d) simulated and (e-h) observed $PM_{2.5}$ concentration (μg m^{-3}) at night, (i-l) the relative bias (RB, %) between simulation and observation, and the calculation formula of relative bias is $RB = \left(\overline{X_{sim}} - \overline{X_{obs}}\right) / \overline{X_{obs}} \times 100\%$, where $\overline{X_{sim}}$ and $\overline{X_{obs}}$ represent the average value of simulation and observation, respectively. The locations of three rivers (i.e., Yellow River, Yangtze-Huaihe and Yangtze River) are marked by blue lines. The red and green dashed circles represent the whole simulation area and Eastern China, respectively. The purple solid irregular circle indicates mountainous areas, and the red text TJ indicates Tianjin.

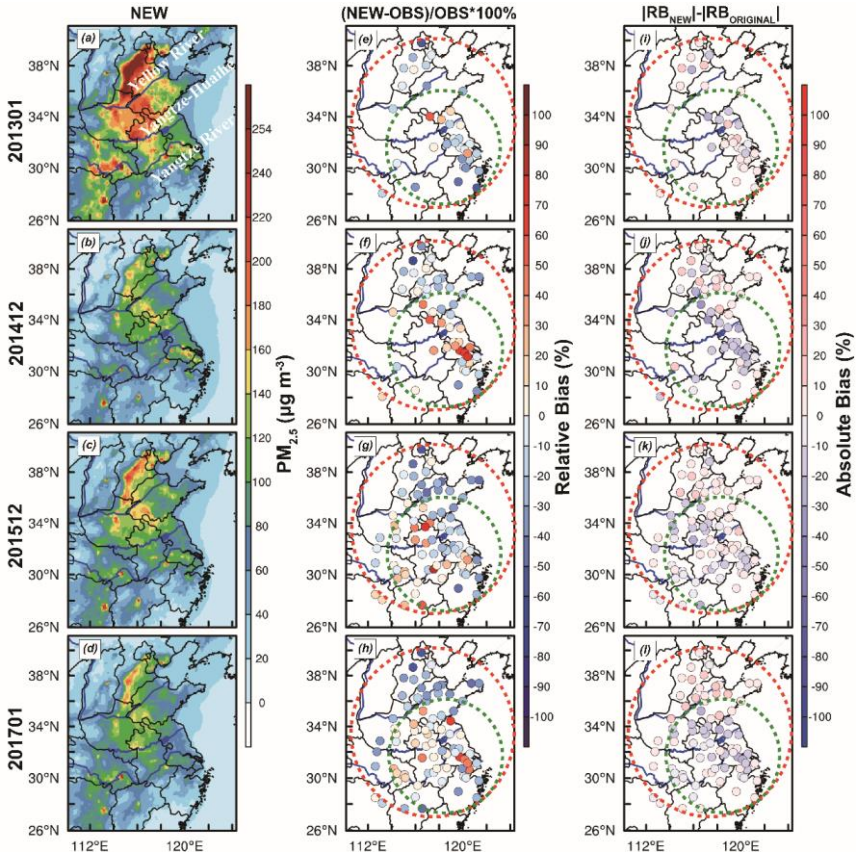

Figure 34. The average value of (a-d) simulated $PM_{2.5}$ concentration (μg m^{-3}) by new schemes, (e-h) the relative bias (RB, %) of $PM_{2.5}$ concentration between simulation of new scheme and observation, (i-l) the absolute bias (AB, %) between new and original schemes, and the calculation formula of absolute bias is $AB = |RB_{new}| - |RB_{original}|$, where $|RB_{new}|$ and $|RB_{original}|$ represent the relative bias of new and original schemes, respectively. The red and green dashed circles represent the whole simulation area and Eastern China, respectively.

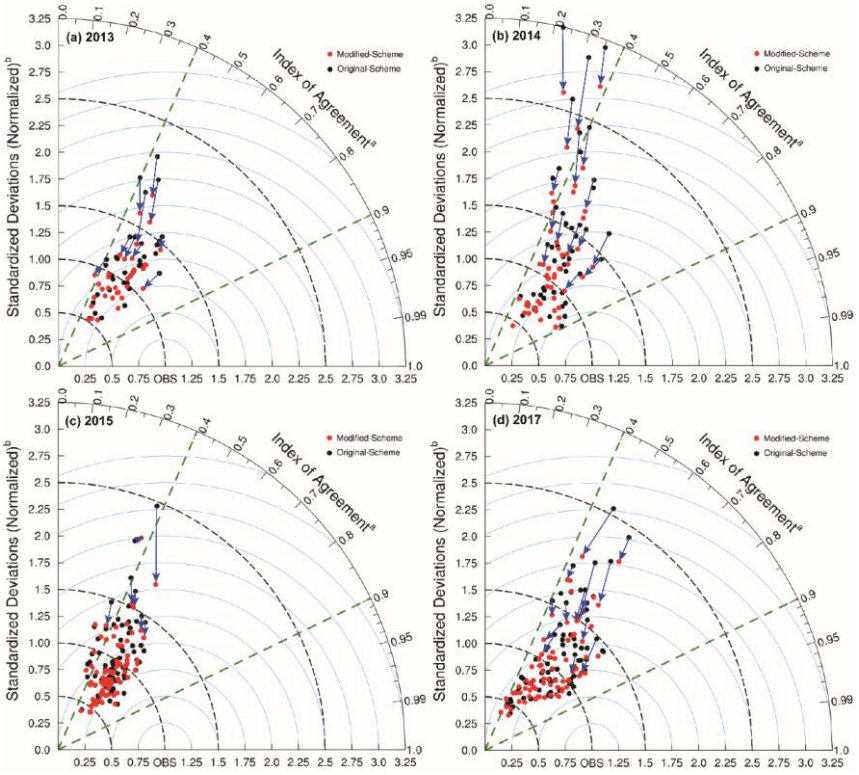

Figure 45. Taylor diagram of simulation by original scheme and modified scheme. XY axes and arc represent the normalized standardized deviations (NSTD, $NSTD = \frac{\sqrt{\frac{1}{N-1}\sum_{i=1}^{n}\left(X_{sim,i} - \overline{X_{sim}}\right)^2}}{\sqrt{\frac{1}{N-1}\sum_{i=1}^{n}\left(X_{obs,i} - \overline{X_{obs}}\right)^2}}$**,** $\overline{X_{sim}}$ **and** $\overline{X_{obs}}$ **represent the average value of simulation and observation, respectively) and index of agreement (IOA,** $IOA = 1 - \frac{\left[\sum_{i=1}^{n} |X_{sim,i} - X_{obs,i}|^2\right]}{\left[\sum_{i=1}^{n} (|X_{sim,i} - \overline{X_{obs}}| + |X_{obs,i} - \overline{X_{obs}}|)^2\right]}$**,** $X_{sim,i}$ **and** $X_{obs,i}$ **represent the value of simulated and observed, respectively. i refers to time and n is the total number of time series), respectively. All cities (a total of 35 cities in 2013 and 78 cities in 2014, 2015 and 2017) are shown through dots, and black (red) represents original (new) scheme. The root mean square (RMS) is denoted by blue dashed line and the arrow indicates the change of the new scheme compared to the original scheme at the same station.**

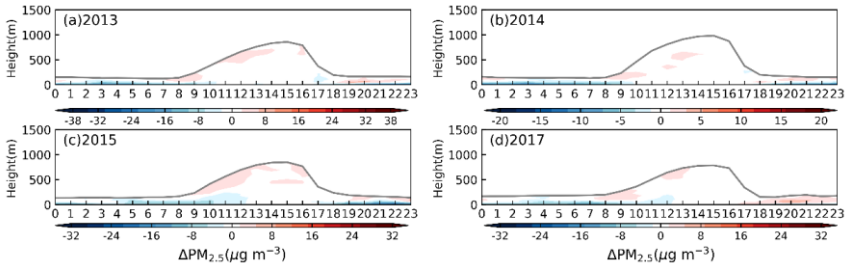

Figure 5~~6~~. Time-height cross sections for the difference of $PM_{2.5}$ concentration between original and new schemes (i.e., the new scheme minus the original scheme) within the PBL. The gray line indicates the PBLH.

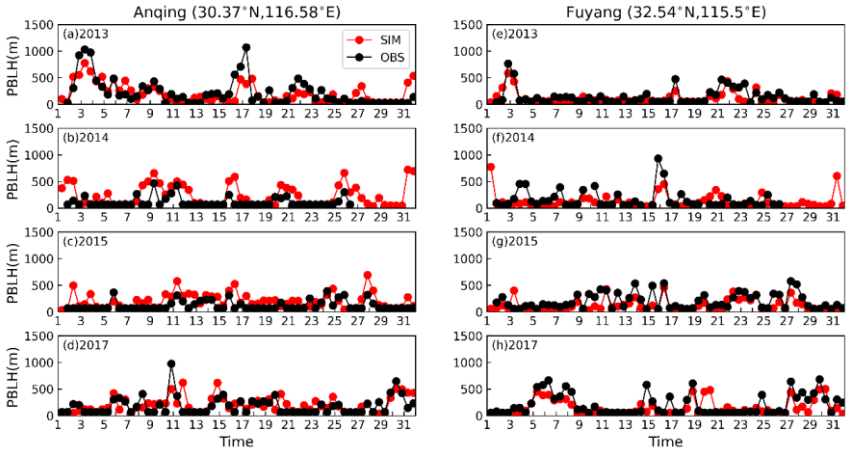

Figure 6~~7~~. Time series of the observed (black) and simulated (red) PBLH at 0800 and 2000 (BJT) in the (a-d) Anqing and (e-h) Fuyang from 2013 to 2017.

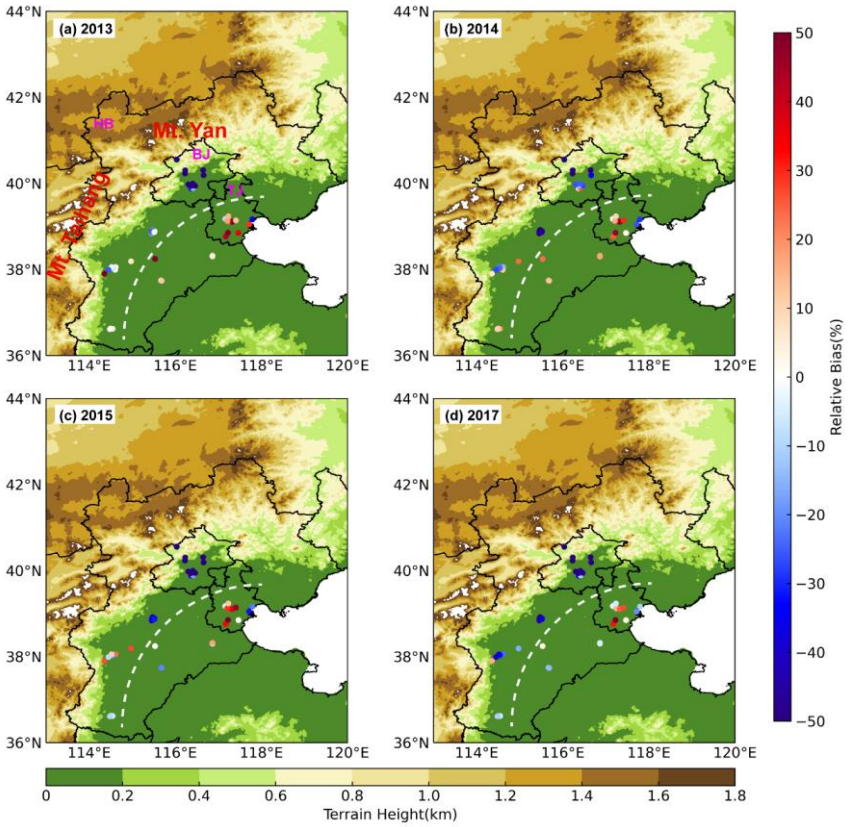

Figure 78. The relative bias (%) between simulation and observation at all environment monitoring stations and terrain height in Beijing-Tianjin-Hebei in (a) 2013, (b) 2014, (c) 2015 and (d) 2017. Taihang Mountain (Mt. Taihang) and Yanshan Mountain (Mt. Yan) are indicated by red text, Beijing (BJ), Tianjin (TJ) and Hebei (HB) are represented by purple abbreviation and the dividing line between overestimated and underestimated areas is indicated by a white dashed line.

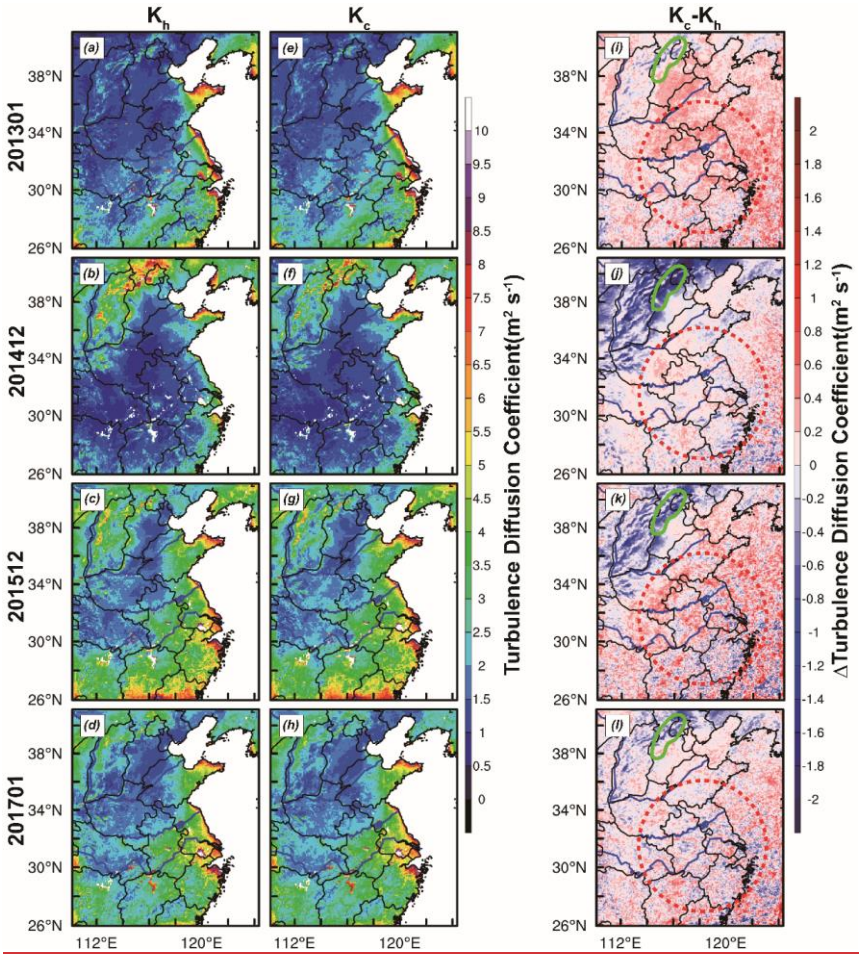

860

Figure 8. Turbulent diffusion coefficient of (a-d) heat and (e-h) particles, and (i-l) the difference between two turbulent diffusion coefficients. The red dashed and green solid irregular circles represent Eastern China and mountainous areas, respectively.

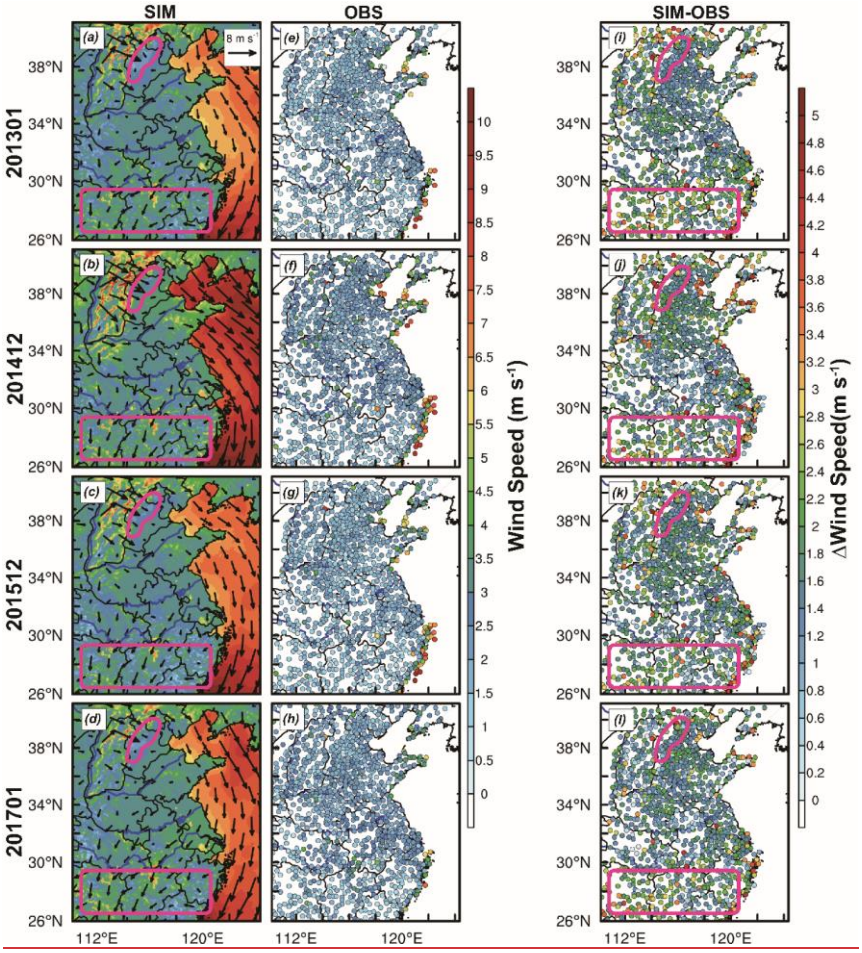

865 **Figure 9. (a-d) Simulated and (e-h) observed wind speed at 10 m above ground level (AGL), and (i-l) the difference of simulated and observed. The purple rectangle indicates the area where the observed wind speed is significantly overestimated.**